Proc. Natl. Acad. Sci. USA
Vol. 88, pp. 6423–6426, August 1991
Biochemistry

Theoretical studies on the dihydrofolate reductase mechanism: Electronic polarization of bound substrates

(local density functional calculations/enzyme catalysis)

JÜRGEN BAJORATH*†, JOSEPH KRAUT‡, ZHENQIN LI*, DAVID H. KITSON*, AND ARNOLD T. HAGLER*§

*Biosym Technologies, Inc., 10065 Barnes Canyon Road, San Diego, CA 92121; and ‡Department of Chemistry, University of California at San Diego, La Jolla, CA 92093

Contributed by Joseph Kraut, April 26, 1991

ABSTRACT **We have applied local density functional theory, an *ab initio* quantum mechanical method, to study the shift in the spatial electron density of the substrate dihydrofolate that accompanies binding to the enzyme dihydrofolate reductase. The results shed light on fundamental electronic effects due to the enzyme that may contribute to catalysis. In particular, the enzyme induces a long-range polarization of the substrate that perturbs its electron density distribution in a specific and selective way in the vicinity of the bond that is reduced by the enzyme. Examination of the electron density changes that occur in folate reveals that a similar effect is seen but this time specifically at the bond that is reduced in this substrate. This suggests that the polarization effect may be implicated in the reaction mechanism and may play a role in determining the sequence whereby the 7,8-bond in folate is reduced first, followed by reduction of the 5,6-bond in the resulting dihydro compound.**

Dihydrofolate reductase (DHFR) catalyzes the NADPH-dependent reduction of folate to 7,8-dihydrofolate and of 7,8-dihydrofolate to 5,6,7,8-tetrahydrofolate (1). We have previously investigated the migration of electron density in folate on binding to DHFR (2) by using local density functional (LDF) calculations (3–10). These calculations showed an increase in σ and a decrease in π electron density in the vicinity of the C-7=N-8 bond of the enzyme-bound pteridine ring, the bond that is reduced, and it was postulated that these changes might be implicated in the enzyme reaction mechanism. Features of the enzyme structure determined to be responsible for this effect included a conserved motif of three positive residues far from the site of reduction, but adjacent to the glutamate moiety of folate. If these specific electronic changes do reflect fundamental aspects of the enzyme mechanism, it follows that a similar σ–π difference electron density pattern ought to be seen in dihydrofolate, a much better substrate, when it binds to the enzyme. In dihydrofolate, however, the N-5=C-6 bond is reduced and one would, therefore, expect to see this difference electron density pattern in the region of the N-5=C-6 bond rather than the C-7—N-8 bond. In the folate study, a σ–π difference electron density pattern comparable to that seen in the region of the C-7=N-8 bond was not seen at the N-5=C-6 bond and it is not obvious why this pattern should be induced around this bond in the dihydro compound since the environment provided by the enzyme molecule is very similar for the two ligands (see below and ref. 11). Thus, to test further the hypothesis based on our previous results and to continue exploring electronic effects that may be related to the catalytic mechanism, we have extended our study to include changes in the spatial electron density distribution of dihydrofolate on binding to DHFR.

The publication costs of this article were defrayed in part by page charge payment. This article must therefore be hereby marked "*advertisement*" in accordance with 18 U.S.C. §1734 solely to indicate this fact.

Difference Electron Density Calculations Using LDF Theory

To explore electronic aspects of DHFR catalysis, we have applied LDF theory, an *ab initio* quantum mechanical method developed in physics (3–6) and recently applied to chemical problems (7–10). The approach used here differs from previous theoretical studies on enzyme mechanisms (12–18) in that it focuses on the accurate calculation and analysis of spatial electron density distributions within the bound substrate molecule, using difference electron density maps to analyze enzyme–substrate interactions. To calculate the spatial electron density distribution of the substrate, both when free and when bound to the enzyme, LDF calculations were carried out with the entire substrate treated quantum mechanically. In the first calculation, the total electron density distribution was obtained for the free substrate molecule in the same conformation as when it is bound. The calculation was then repeated in the electrostatic field of the hydrated holoenzyme (enzyme plus cofactor) by incorporating the electrostatic potential due to the enzyme–cofactor complex into the Hamiltonian of the substrate. From the results of the two calculations, the difference electron density (bound − free) was calculated and examined with the aid of computer graphics.

Computational Details

All LDF calculations described here were carried out using the DMOL program (Biosym Technologies, San Diego). A vectorized version of the program was run on Cray Y-MP supercomputers. For the quantum mechanical calculations on dihydrofolate a numerical basis set with polarization functions, equivalent in size to a Gaussian 6-31G** basis set, was used. Dihydrofolate has 51 atoms (32 nonhydrogen), which corresponds to 543 orbitals in the representation used here (including the 1s orbitals on the nonhydrogen atoms, which were frozen during the calculation). The charge density of dihydrofolate used for difference electron density calculations and an atomic population analysis were computed at the level of the self-consistent LDF solution. The convergence criterion for the calculation was an rms change in density for one step (calculated over all grid points) of <0.0001 electron per Bohr^3 (1 Bohr $\approx$ 0.53 Å, a Bohr radius). In the calculation of bound dihydrofolate, the point charges at the positions of each of the enzyme, cofactor, and water atoms were included in the effective Hamiltonian for the LDF calculation as a corresponding Coulombic potential. The self-consistent LDF solution with this additional potential then gave the charge density of the bound substrate. For each of the quantum mechanical

Abbreviations: DHFR, dihydrofolate reductase; LDF, local density functional.

†Present address: Bristol-Myers Squibb, Pharmaceutical Research Institute–Seattle, 3005 1st Avenue, Seattle, WA 98121.
§To whom reprint requests should be addressed.

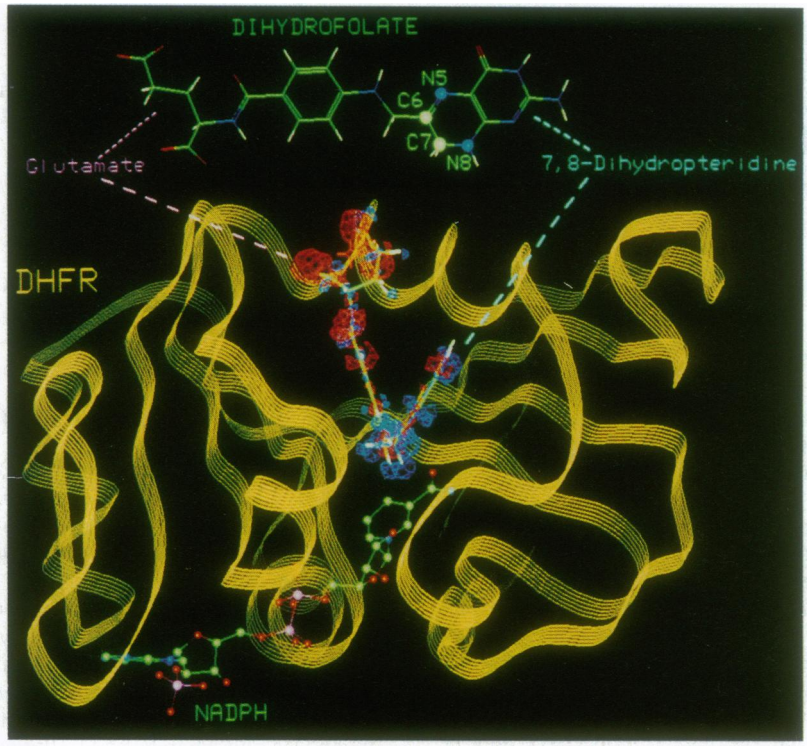

FIG. 1. Long-range polarization of dihydrofolate induced by binding to DHFR. A schematic representation of dihydrofolate is shown as a reference. The polarization is illustrated by difference electron density contours (bound − free) at two levels: 0.002 electron/Bohr^3 (e/B^3) (red) (i.e., these regions gain electron density and become more negative upon binding); and −0.002 e/B^3 (blue) (these regions become more positive upon binding). As can be seen, upon binding, electron density migrates from the dihydropteridine ring to the glutamate moiety of the substrate dihydrofolate.

calculations on bound and free dihydrofolate reported here, 1–7 hr of computer time, depending on the convergence behavior, was needed on the Cray Y-MP.

Model of the Ternary Complex DHFR–NADPH–Dihydrofolate

The ternary complex of the ground state DHFR–NADPH–dihydrofolate was modeled based on the ternary complex DHFR–NADPH–folate (2) that was derived from the crystal structure of the corresponding *Escherichia coli* DHFR complex with folate and NADP$^+$ (11). The model includes a 5- to 8-Å hydration layer around the ternary complex. Model building on the dihydrofolate complex was carried out as suggested by Bystroff *et al.* (11), followed by a constrained energy minimization protocol (2). For all nonhydrogen protein atoms the overall rms difference in atomic positions between the DHFR–NADPH–folate and the DHFR–NADPH–dihydrofolate complexes is 0.26 Å after the energy minimization procedure. The final rms positional difference between corresponding atoms in dihydrofolate and folate (including calculated hydrogens) is only 0.20 Å. Comparison of the resulting structure with the folate complex revealed the formation of a hydrogen bond between N-8 of the 7,8-dihydropteridine ring and the carbonyl oxygen of Ile-5. This was accomplished by a slight rotation of the dihydropteridine ring and a slight shift in the position of the carbonyl oxygen of Ile-5. The formation of this hydrogen bond is the only major additional feature of the protein–ligand interaction in the case of dihydrofolate. The same additional interaction was found in the crystal structure of a complex between 5-deazafolate and recombinant human DHFR (19).

Long-Range Polarization of Dihydrofolate

Our calculations show that, under the influence of the enzyme's electrostatic environment, bound dihydrofolate undergoes a long-range polarization over its entire length of ≈18 Å (Fig. 1). The effect is similar in magnitude and direction to the polarization calculated for folate (2) (Table 1). In the case of folate, 0.61 unit of electron charge is shifted from the pteridine ring to the glutamate moiety, and in dihydrofolate the glutamate moiety accepts 0.53 electron charge. Direct electrostatic interactions with specific conserved protein residues give rise to ≈65% of the polarization, while ≈35% is due to electrostatic effects arising from the rest of the holoenzyme molecule (2). These specific interactions can be related to the electrostatic potential of DHFR in solution (21).

Changes in the Electron Density of the 7,8-Dihydropteridine Ring

Especially pronounced changes in electron density are observed in the vicinity of certain atoms and bonds of the 7,8-dihydropteridine ring system upon binding to the enzyme (Fig. 2 *Left*). In particular, the overall difference electron density around N-5 and C-6 shows that this is the most

Table 1. Charge migration induced in dihydrofolate and folate on binding to DHFR

	Charge				Δ charge (bound − free)	
	Free		Bound			
Fragment	DHF	Folate	DHF	Folate	DHF	Folate
"Pteridine"	−0.30	−0.42	+0.17	+0.19	+0.47	+0.61
pABA	−0.26	−0.26	−0.21	−0.26	+0.05	+0.00
Glutamate	−1.43	−1.32	−1.97	−1.93	−0.53	−0.61

The total net charge on each fragment is given, calculated by summing the individual atomic charges determined from a Mulliken population analysis (20). The fragment "pteridine" represents 7,8-dihydropteridine in dihydrofolate (DHF) and pteridine in folate. Additional calculations reveal that the presence of the hydration shell and the cofactor have only a slight shielding effect on the polarization (<10%). pABA, *p*-aminobenzoic acid.

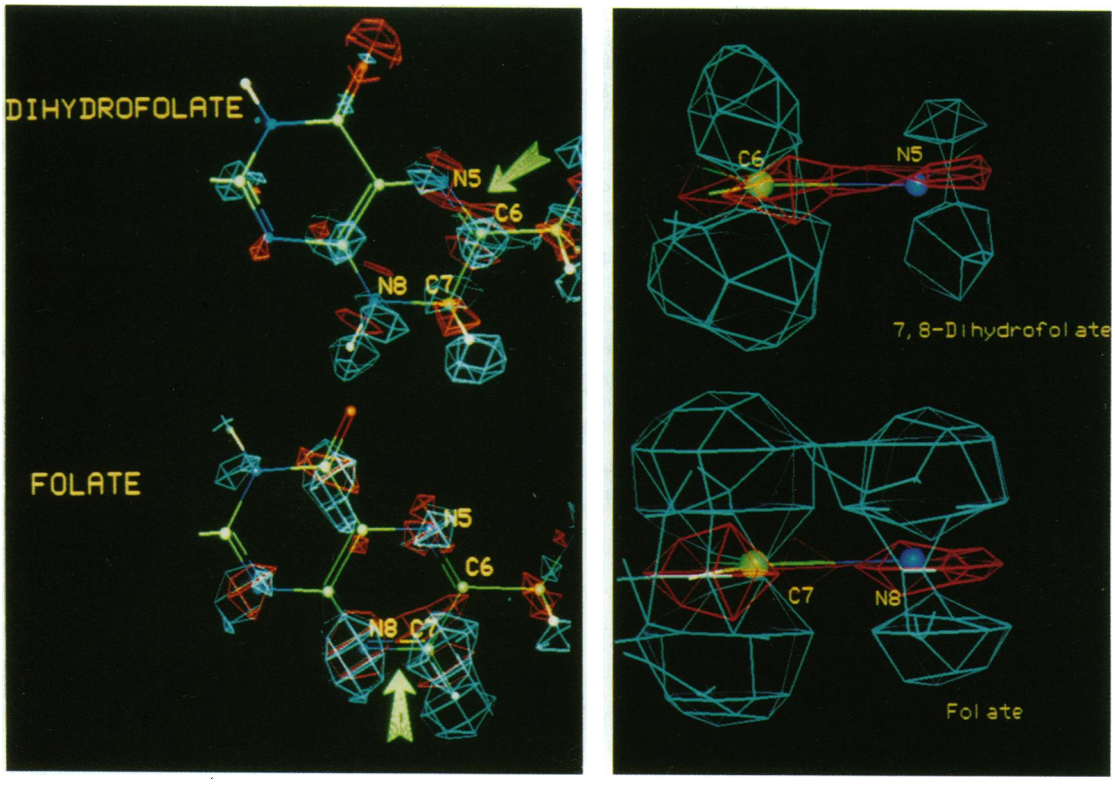

FIG. 2. (*Left*) Difference electron density in the 7,8-dihydropteridine ring of the substrate dihydrofolate, illustrating the electron density redistribution in the substrate on binding to DHFR. Contours are shown as described in Fig. 1. Significant changes can be seen in the vicinity of the N-5=C-6 bond, which is reduced on going from dihydrofolate to tetrahydrofolate. In contrast, in the case of folate, the region in the vicinity of the C-7=N-8 double bond is predominantly affected. The carbonyl oxygen of the dihydropteridine ring (O-4) in dihydrofolate also shows a significant increase in electron density, whereas O-4 is virtually unaffected in the pteridine ring of folate. (*Right*) Difference electron density through the N-5=C-6 double bond in dihydrofolate and the C-7=N-8 double bond in folate in a plane perpendicular to the pteridine ring. A clear difference is revealed between the perturbation of the density in the region of the two bonds in the plane of the pteridine ring and above and below the plane. At the σ electron level, a more negative charge is developed upon binding to the enzyme, while, conversely, the π electrons become depleted and the out-of-plane region becomes more positive.

significantly affected double bond in the dihydropteridine ring. The N-5=C-6 double bond is the bond that is reduced on going from 7,8-dihydrofolate to 5,6,7,8-tetrahydrofolate. A clear separation of the difference electron density in the vicinity of N-5 and C-6 can be observed (Fig. 2 *Right*), with an increased electron density developed at the σ level, in the ring plane, while the π electron density above and below the ring plane is diminished. As Fig. 2 shows, these changes are similar to those that take place in the region of the C-7=N-8 bond in the folate system.

The major difference between the enzyme–ligand interactions of bound folate and dihydrofolate, as discussed above, is an additional hydrogen bond between the HN-8 of the dihydropteridine ring and the carbonyl oxygen of Ile-5. To determine whether this hydrogen bond is responsible for the differences between the electron density changes in the folate and dihydrofolate systems, further LDF calculations on bound dihydrofolate, with all partial charges on Ile-5 omitted, were carried out. These revealed that the electrostatic contribution of this hydrogen bond is not itself responsible for the difference in the selective electron density changes in the region of the reactive bonds in the pteridine rings of folate and dihydrofolate. Thus, the specific electron density changes of folate and dihydrofolate that take place upon binding would seem to arise through intrinsic molecular properties of the substrates in their binding conformation.

Implications for the Reaction Mechanism of DHFR and Order of Reduction

Our calculations show that in folate the charge density in the region of the C-7=N-8 bond is perturbed, resulting in an overall diminution of π electron density and a slight increase in σ electron density. In dihydrofolate, the region around the N-5=C-6 bond is selectively influenced in the same manner. That the difference electron density pattern is seen specifically in the vicinity of the bond that is reduced in folate, and that it is then "transferred" to the bond that is reduced in dihydrofolate, strongly suggests that this effect could be significant for the reaction mechanism of the enzyme. These results, therefore, demonstrate how the electrostatic field of the enzyme may be inducing changes in the substrate that play a role in the reduction reaction.¶ Furthermore, the results indicate that these effects may be involved in determining the sequence of the reactions catalyzed by DHFRs (i.e., that the 7,8-bond in folate is reduced first, followed by reduction of the 5,6-bond in the resulting dihydro compound).

Another striking feature of the difference electron density maps for dihydrofolate is the enhanced electron density at O-4 (Fig. 2 *Left*). This is especially suggestive, as it is thought that intermediate protonation at O-4 is mechanistically important for the protonation at N-5 in the transition state of dihydrofolate (11). Such an effect is not seen for folate, where N-5 protonation is not required for reduction.

¶We had previously postulated that the changes in the σ and π electron densities that are seen around the bonds that are reduced might correspond to a reduction in double-bond character. Preliminary analysis of overlap populations calculated to explore this qualitative assessment suggests alternative interpretations of the electron migrations. Further details of this aspect of the work will be published elsewhere.

We thank Prof. Dennis Salahub (University of Montreal) and Dr. Michael Wrinn (Biosym Technologies) for helpful discussions. Financial support was provided by the National Institutes of Health (Grant GM30564) and computer time was provided by the San Diego Supercomputer Center, the National Center for Supercomputing Applications, and Cray Research, Inc.

1. Kraut, J. & Matthews, D. A. (1987) in *Biological Macromolecules and Assemblies*, eds. Jurnak, F. A. & McPherson, A. (Wiley, New York), Vol. 3, pp. 1–72.
2. Bajorath, J., Kitson, D. H., Fitzgerald, G., Andzelm, J., Kraut, J. & Hagler, A. T. (1991) *Proteins: Struct. Funct. Genet.* **9**, 217–224.
3. Hohenberg, P. & Kohn, W. (1964) *Phys. Rev. B* **136**, 864–871.
4. Kohn, W. & Sham, L. J. (1965) *Phys. Rev. A* **140**, 1133–1138.
5. Delley, B. & Ellis, D. E. (1982) *J. Chem. Phys.* **76**, 1949–1960.
6. Parr, R. G. & Yang, W. (1989) *Density-Functional Theory of Atoms and Molecules* (Oxford Univ. Press, New York).
7. Parr, R. G. (1983) *Annu. Rev. Phys. Chem.* **34**, 631–656.
8. Kutzler, F. W., Swepston, P. N., Berkovitch-Yellin, Z., Ellis, D. E. & Ibers, J. A. (1983) *J. Am. Chem. Soc.* **105**, 2996–3004.
9. Delley, B. (1986) *Chem. Phys.* **110**, 329–338.
10. Krijn, M. P. C. M. & Feil, D. (1988) *J. Chem. Phys.* **89**, 4199–4208.
11. Bystroff, C., Oatley, S. J. & Kraut, J. (1990) *Biochemistry* **29**, 3263–3277.
12. Warshel, A. & Levitt, M. (1976) *J. Mol. Biol.* **103**, 227–249.
13. Tapia, O. & Johannin, G. (1981) *J. Chem. Phys.* **75**, 3624–3635.
14. Alagona, G., Desmeules, P., Ghio, C. & Kollman, P. A. (1984) *J. Am. Chem. Soc.* **106**, 3623–3632.
15. Lambros, S. A., Richards, W. G. & Marchington, A. F. (1984) *J. Mol. Struct. (Theochem.)* **109**, 61–71.
16. Weiner, S. J., Seibel, G. L. & Kollman, P. A. (1986) *Proc. Natl. Acad. Sci. USA* **83**, 649–653.
17. Rullmann, J. A. C., Bellido, M. N. & van Duijnen, P. T. (1989) *J. Mol. Biol.* **206**, 101–118.
18. Warshel, A., Sussman, F. & Hwang, J.-K. (1989) *J. Mol. Biol.* **201**, 139–159.
19. Davies, J. F., Delcamp, T. J., Prendergast, N. J., Ashford, V. A., Freisheim, J. H. & Kraut, J. (1990) *Biochemistry* **29**, 9467–9479.
20. Mulliken, R. S. (1955) *J. Chem. Phys.* **23**, 1833–1840.
21. Bajorath, J., Kitson, D. H., Kraut, J. & Hagler, A. T. (1991) *Proteins: Struct. Funct. Genet.*, in press.